

1990016914

QPSK Loop Lock Detection in the Advanced Receiver

A. Mileant

Telecommunications Systems Section

S. Hinedi

Communications Systems Research Section

The Advanced Receiver (ARX II) currently being developed uses a Costas cross-over loop to acquire and track the phase of an incoming quadrature phase-shift-keyed (QPSK) signal. This article describes the performance of the QPSK lock detector to be implemented, taking into account the phase jitter in the tracking loop. Simulations are used to verify the results of the analysis.

I. Introduction

The Advanced Receiver II (ARX II) [1] is currently being developed to demodulate signals from deep space spacecraft. In addition to processing binary phase-shift-keyed (BPSK) signals, the ARX II will acquire and track quadrature phase-shift-keyed (QPSK) signals. The tracking as well as the acquisition performance of several QPSK loops has been investigated [2], and it was determined that the Costas cross-over loop offered a "good" compromise between implementational complexity and relative performance. The other two candidates were the maximum a posteriori (MAP) estimation and the generalized Costas loops. This article describes a lock detector for the QPSK loops. The analysis is general in that it is applicable to all three QPSK loops, and the results are validated by computer simulations. The general QPSK carrier-tracking loop structure and the lock detector are both shown in Fig. 1. When this loop is implemented, an extra accumulator is present in front of the loop filter to reduce the loop update rate and improve the loop signal-to-noise ratio (SNR). The lock detector structure can be gener-

alized to accommodate any multiple phase-shift-keying (MPSK) signal as described in [3].

II. Lock Detection Analysis

The received QPSK signal can be modeled by

$$r(t) = \sqrt{P_D}a(t)\sin(\omega_0 t + \theta) + \sqrt{P_D}b(t)\cos(\omega_0 t + \theta) + n(t) \quad (1)$$

where

$$a(t) = \sum_k a_k p(t - kT_s)$$

and

$$b(t) = \sum_k b_k p(t - kT_s)$$

are the independent in-phase and quadrature data streams with a_k and b_k the binary ± 1 random data and $p(t)$ the

non-return-to-zero (NRZ), or Manchester, pulse of duration over T_s seconds. The data power is given by P_D and the incoming phase by θ . The signal is received in the presence of noise that can be expressed as

$$n(t) = \sqrt{2}n_c(t)\cos(\omega_0 t + \theta) - \sqrt{2}n_s(t)\sin(\omega_0 t + \theta) \quad (2)$$

where $n_c(t)$ and $n_s(t)$ are random processes with a two-sided noise spectral density of $N_0/2$. The input signal is mixed with the reference signals

$$x_c(t) = \frac{2\sqrt{P_D}}{N_0} \cos(\omega_0 t + \hat{\theta}) \quad (3a)$$

and

$$x_s(t) = \frac{2\sqrt{P_D}}{N_0} \sin(\omega_0 t + \hat{\theta}) \quad (3b)$$

to produce, after integrating and dumping, the samples

$$\begin{aligned} r_{sk} &= \int_{kT_s}^{(k+1)T_s} r(t)x_s(t) dt \\ &= R \left(a_k \cos \phi - b_k \sin \phi - \frac{x_{1k}}{\sqrt{R}} \cos \phi - \frac{x_{2k}}{\sqrt{R}} \sin \phi \right) \\ r_{ck} &= \int_{kT_s}^{(k+1)T_s} r(t)x_c(t) dt \\ &= R \left(a_k \sin \phi + b_k \cos \phi - \frac{x_{1k}}{\sqrt{R}} \sin \phi + \frac{x_{2k}}{\sqrt{R}} \cos \phi \right) \end{aligned} \quad (4)$$

where $R \triangleq \frac{P_D T_s}{N_0}$ is the symbol SNR, x_{1k} and x_{2k} are two zero-mean, independent white Gaussian random sequences with unity variance, and $\phi \triangleq \theta - \hat{\theta}$ is the phase estimation error. The reference signals of Eq. (3a) and Eq. (3b) need to be normalized by $\sqrt{P_D}/N_0$ for only the MAP estimation loop, which contains the "hyperbolic tangent" nonlinearity. For the other two loops, the amplitude can be a constant independent of $\sqrt{P_D}/N_0$. The tracking performance of the three QPSK tracking loops has been derived elsewhere [3], and the results are summarized in Appendix A.

The lock detector algorithm used in the ARX II is summarized in Appendix B for a general MPSK signal. In the specific case of a QPSK signal, the algorithm reduces to

$$z = \sum_{k=1}^M y_k \gtrless \tau \quad (5a)$$

where z is the detector's signal obtained from samples y_k

$$y_k \triangleq (r_{ck}^2 - r_{sk}^2)^2 - (2r_{ck}r_{sk})^2 \quad (5b)$$

It is shown in Appendix C that the mean and the variance of the detector signal z can be expressed as

$$\mu_z = -4MR^4 \overline{\cos 4\phi} \quad (6a)$$

and

$$\begin{aligned} \sigma_z^2 &= 2M \left[m_8 + 19m_{44} - 12m_{62} \right] \\ &+ 4M \left[\frac{1}{M} \sum_{k=1}^{M-1} c_k d_k - Mm_4^2 - 9m_2^4 + 6m_4 m_2^2 \right] \end{aligned} \quad (6b)$$

where ϕ denotes the carrier phase error; $m_i = \mathbf{E}\{r_c^i\} = \mathbf{E}\{r_s^i\}$ the i th moment; $m_{ij} = \mathbf{E}\{r_c^i r_s^j\}$ the ij th cross-moment; and c_k, d_k are constants defined in Appendix C. (The overbar and \mathbf{E} indicate expected values.) Note that at high-loop SNR (i.e., when $\sigma_\phi \rightarrow 0$), the mean and variance reduce to

$$\mu_z = -4MR^4 \quad (7a)$$

and

$$\sigma_z^2 = 64MR^8 \left[\frac{2}{R} + \frac{9}{R^2} + \frac{12}{R^3} + \frac{3}{R^4} \right] \quad (7b)$$

from which the ideal detector's SNR can be derived. At lower loop SNRs, the phase jitter might not be negligible and might result in a degraded detector SNR. All the derivations have been summarized in Appendix C for reference.

III. Probability of Detection and of False Indication

During carrier lock detection, each z sample is compared with a predefined threshold τ , and the lock detector decides that the loop is in-lock when z exceeds τ (i.e., $z > \tau$). It is possible that even when the loop is still not locked or when no signal is present, z will occasionally be larger than τ . In this case, the lock detector will mistakenly declare an in-lock condition. The probability of this event (probability of false indication) is

$$P_f = \frac{1}{\sqrt{2\pi\sigma_{z0}^2}} \int_{\tau}^{\infty} \exp\left(-\frac{(z - \mu_{z0})^2}{2\sigma_{z0}^2}\right) dz$$

$$= \frac{1}{2} \operatorname{erfc}\left(\frac{\tau - \mu_{z0}}{\sqrt{2\sigma_{z0}^2}}\right) \quad (8)$$

where μ_{z0} and σ_{z0}^2 are the mean and variance of the lock detector signal in the out-of-lock state and $\operatorname{erfc}(x)$ is the complementary error function ($\operatorname{erfc}(x) = 1 - \operatorname{erf}(x)$, where $\operatorname{erf}(x)$ is the error function). Equation (8) assumes that z is a Gaussian random variable since z is the sum of many samples of equal variance. When the loop is not locked on the signal, the input can be modeled as pure noise to produce

$$\mu_{z0} = 0 \quad (9)$$

$$\sigma_{z0}^2 = 192MR^4$$

On the other hand, when the loop is locked on the signal, the probability of detection is given by

$$P_d = \frac{1}{\sqrt{2\pi\sigma_z^2}} \int_{\tau}^{\infty} \exp\left(-\frac{(z - \mu_z)^2}{2\sigma_z^2}\right) dz$$

$$= \frac{1}{2} \operatorname{erfc}\left(\frac{\tau - \mu_z}{\sqrt{2\sigma_z^2}}\right) \quad (10)$$

where μ_z and σ_z^2 are given by Eq. (6). Alternatively, the threshold can be eliminated from Eq. (10) and the probability of detection expressed as

$$P_d = \frac{1}{2} \operatorname{erfc}\left(\frac{\sigma_{z0}}{\sigma_z} \operatorname{erfc}^{-1}(2P_f) - \sqrt{\frac{SNR_z}{2}}\right) \quad (11)$$

where $SNR_z = \mu_z^2/\sigma_z^2$ denotes the detector SNR. The phase jitter in the tracking loop degrades the detector's SNR by a factor D ,

$$D = \frac{SNR_z}{SNR_{z,ideal}} \quad (12)$$

where $SNR_{z,ideal}$ is the detector SNR if an infinite-loop SNR is assumed; i.e., there is no phase jitter ($SNR_{z,ideal}$ is computed by using the high-SNR approximations for μ_z and σ_z^2 given by Eq. (7)). In Appendix A, it is shown that at high-loop SNR the detector's SNR reduces to

$$SNR_{z,ideal} = \frac{MR}{4(2 + \frac{9}{R} + \frac{12}{R^2} + \frac{3}{R^3})} \quad (13)$$

For a given M , loop SNR, ρ , ($\rho = 1/\sigma_{\phi}^2$ where σ_{ϕ}^2 is given by Eq. (A-13)), and P_f , the detector's SNR, has to be increased roughly by the factor $1/D$ in order to achieve the desired probability of detection P_d .

Given P_d and P_f , we can solve for the number of required detector samples M , namely,

$$M = \frac{2}{\mu_y^2} \left[\sigma_{y0} \operatorname{erfc}^{-1}(2P_f) - \sigma_y \operatorname{erfc}^{-1}(2P_d) \right]^2 \quad (14)$$

The threshold τ is obtained by solving Eq. (8) and setting it equal to

$$\tau = \sqrt{2\sigma_{z0}^2} \operatorname{erfc}^{-1}(2P_f) \quad (15)$$

where $\operatorname{erfc}^{-1}(\cdot)$ is the inverse complementary error function. When the loop is in lock, it can be argued via the central-limit theorem that the random variable z is approximately Gaussian, with mean and variance as obtained earlier.

IV. Discussion and Numerical Results

Computer simulations were used to validate the various assumptions made in the analysis. Figure 2 depicts the detection probability as a function of loop SNR when $P_f = 10^{-4}$. It is clear that the detection probability degrades significantly at low-loop SNR and the degradation itself is a function of the desired detection probability $\overline{P_d}$ (which is computed assuming zero phase jitter). The degradation is better shown in Fig. 3, which depicts the loss in detector SNR as a function of the loop SNR. At 20-dB loop SNR, the degradation is about 1 dB, but it increases to 2.5 dB as the loop SNR is reduced to 15 dB. In both figures, the simulations and theory are in agreement for all three loops. Note that the degradation in detector SNR for BPSK was about 1 dB for 15-dB loop SNR [5].

When the detection probability was plotted as a function of symbol SNR, different performances for the various loops were expected, as the loop SNRs are different when both the data rate and the loop bandwidth are fixed. Figure 4 clearly depicts that effect, as the MAP estimation loop attains a higher detection probability than the Costas cross-over loop because of its higher loop SNR. Finally, Fig. 5 shows both the nominal and the actual (16-dB loop SNR) detection probabilities as a function of the number of samples M and the corresponding threshold. This kind of curve is very useful when one is designing the operating parameters of the lock detector.

Figure 6 depicts the probability of detection versus the detector's SNR for several values of probability of false lock. This figure is useful in determining the required detector's SNR for a desired detector's performance. Finally, Fig. 7 plots the detector's SNR versus E_s/N_0 for $M = 300$. The detector's SNR for other values of M can be computed from the following relation:

$$SNR_{z,M} = SNR_{z,300} + 10 \log_{10} \left(\frac{M}{300} \right) \text{ dB} \quad (16)$$

As a design example, suppose that a QPSK detector operates at $P_f = 10^{-4}$ and $P_d = 0.99$, and that the signal rate is 10,000 symbols per second with $E_s/N_0 = 1.0$ dB. Using Fig. 6, it can be seen that the detector's SNR should be about 12 dB. But, Fig. 7 states that at $E_s/N_0 = 1$ dB, $M = 300$ and loop SNR = 16 dB (low-loop SNR case), the detector's SNR will actually be about 5.0 dB. Equa-

tion (16) is used to compute the number of samples, M , required to achieve 12 dB of the detector's SNR, which results in $M = 300 \times 10^{(12-5.0)/10} = 1504 = 0.15$ sec, and Eq. (15) is used to compute the threshold τ needed for $P_f = 10^{-4}$. Alternatively, Fig. (5) can be used to find the required threshold value, which turns out to be $\tau = 1300$, assuming that the output of the integrate-and-dump devices is scaled by $1.0/(E_s/N_0)$.

V. Conclusion

This article analyzed the lock detector performance for the QPSK carrier-tracking loop in the ARX II. The analysis is general and is applicable to other QPSK loops. Both analysis and simulation were used to show that the effect of phase jitter on the detector SNR can be significant (as much as two decibels), especially at low-loop SNR.

References

- [1] S. Hinedi, "A Functional Description of the Advanced Receiver," *TDA Progress Report 42-100*, vol. October-December 1989, Jet Propulsion Laboratory, Pasadena, California, pp. 131-149, February 15, 1990.
- [2] S. Hinedi and B. Shah, "QPSK Carrier-Acquisition Performance in the Advanced Receiver II," *TDA Progress Report 42-100*, vol. October-December 1989, Jet Propulsion Laboratory, Pasadena, California, pp. 150-159, February 15, 1990.
- [3] W. Lindsey and M. Simon, *Telecommunications Systems Engineering*, Englewood Cliffs, New Jersey: Prentice Hall, 1973.
- [4] M. K. Simon, "Further Results on Optimum Receiver Structure for Digital Phase and Amplitude Modulated Signals," *Conference Record: 1978 International Conference on Communications*, Toronto, Canada, pp. 42.1.1-1.7, June 4-7, 1978.
- [5] A. Mileant and S. Hinedi, "Costas Loop Lock Detection in the Advanced Receiver," *TDA Progress Report 42-99*, vol. July-September 1989, Jet Propulsion Laboratory, Pasadena, California, pp. 72-89, November 15, 1989.

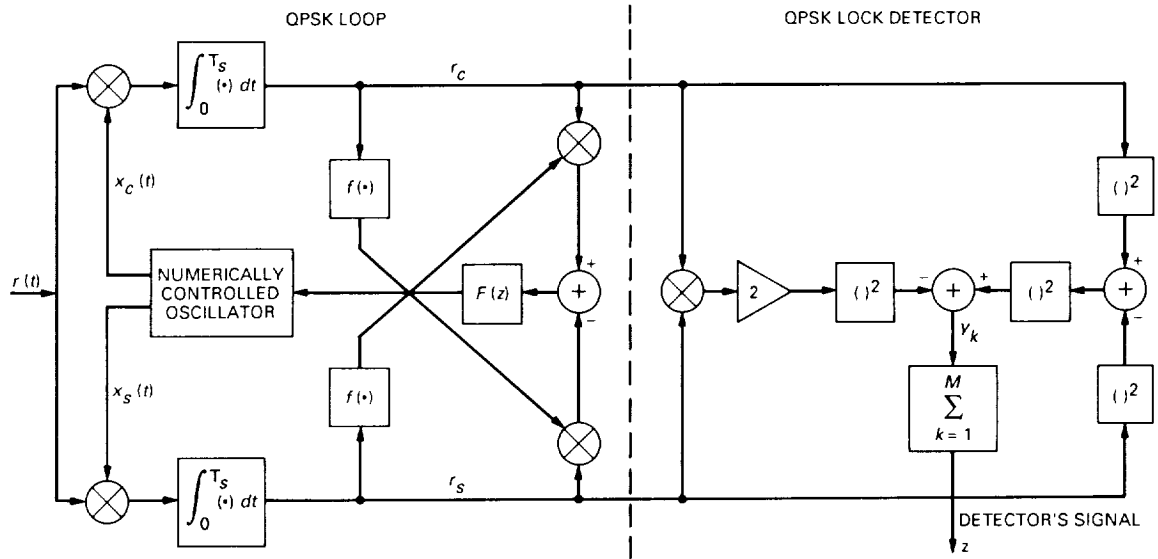


Fig. 1. Implementation of the QPSK loop with lock detector.

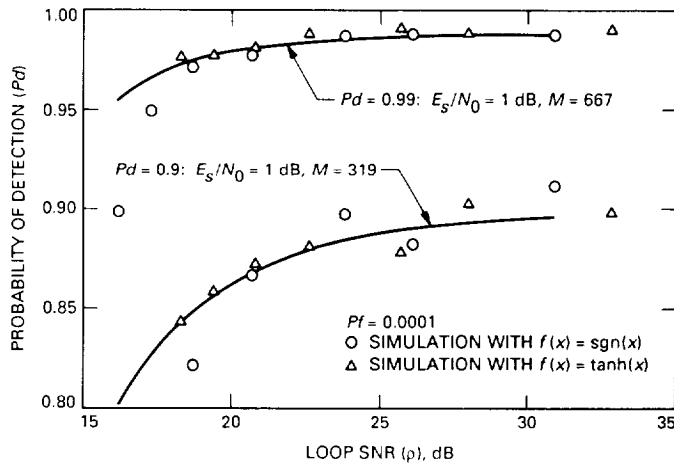


Fig. 2. Probability of detection versus loop SNR.

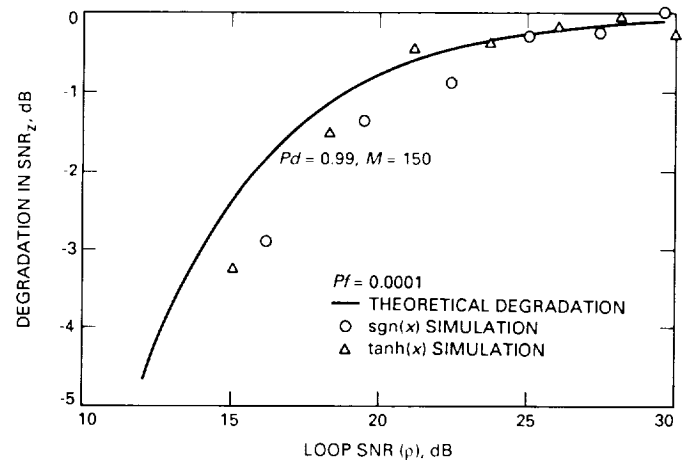


Fig. 3. Degradation in detector SNR versus loop SNR.

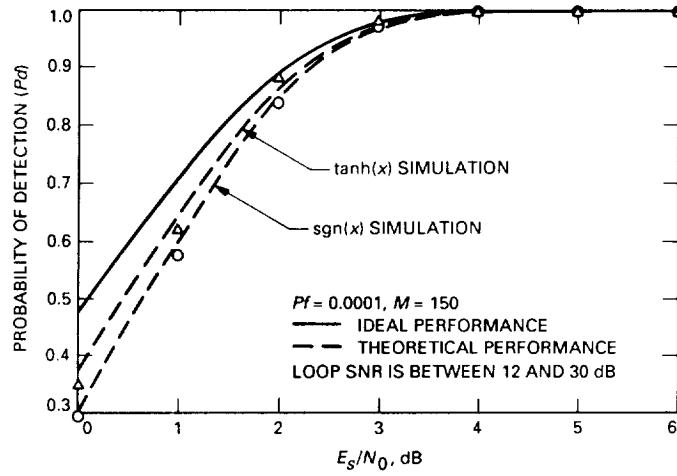


Fig. 4. Probability of detection versus E_s/N_0 . (Theoretical performance assumes degradation due to phase jitter in the loop.)

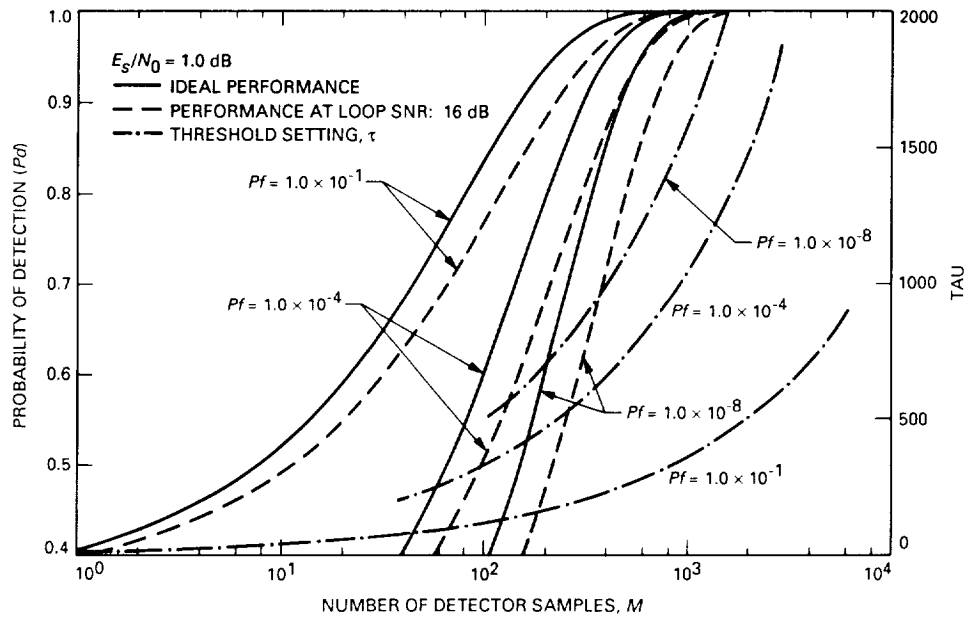


Fig. 5. Probability of detection versus number of detector samples. (The values of τ are given with the assumption that the outputs of the integrate-and-dump devices are scaled by $1/(E_s/N_0)$.)

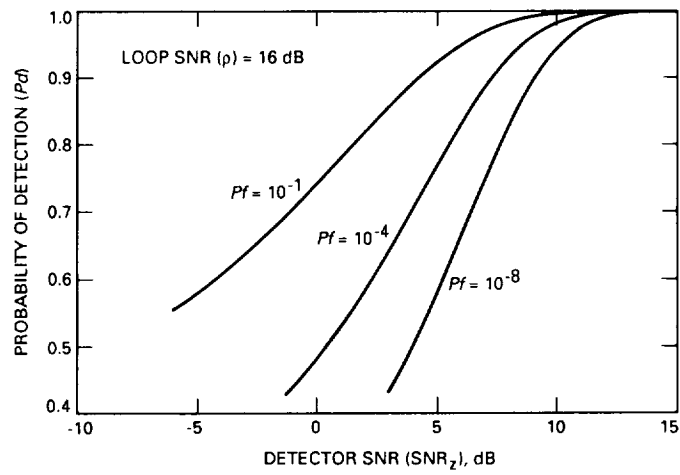


Fig. 6. Probability of detection versus detector SNR.

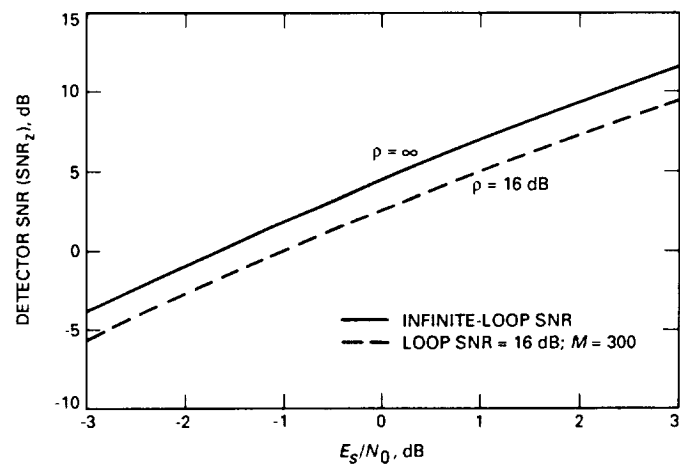


Fig. 7. Detector SNR versus E_s/N_0 .

Appendix A

Tracking Performance of Three QPSK Carrier Loops

Depending on the loop, the samples r_c and r_s of Eq. (4) are processed to produce the error signal that forms the input to the loop filter. In general, that error signal can be expressed as

$$\epsilon(\phi) = r_{ck}f(r_{sk}) - r_{sk}f(r_{ck}) \quad (\text{A-1})$$

where $f(x)$ is some nonlinear odd function that defines the loop. Three possible functions will be considered:

$$f(x) = \begin{cases} \text{sgn}(x) \\ x^3 \\ \tanh(x) \end{cases} \quad (\text{A-2})$$

In order to predict the performance of the loops, we need to compute the “squaring loss,” S_L , which is defined by

$$S_L \triangleq \frac{(\mathbf{E}\{\epsilon'(0)\})^2}{\mathbf{E}\{\epsilon^2(0)\}} \quad (\text{A-3})$$

where $\epsilon(0)$ and $\epsilon'(0)$ are the error signal and its slope, respectively, evaluated at $\phi = 0$. Note that $\mathbf{E}\{\epsilon^2(0)\} = \overline{N^2}$ equals the variance of the open-loop phase error process, σ_N^2 . From this, one obtains the equivalent single-sided noise spectral density, N'_0 , using the relation $N'_0 = 2\overline{N^2}T_s$, where T_s is the symbol time. The loop responds to the mean of the error signal, which is given by

$$\begin{aligned} \overline{\epsilon(\phi)} = & \mathbf{E} \left\{ R(a_k \sin \phi + b_k \cos \phi) f \left[R \left(a_k \cos \phi - b_k \sin \phi + (-x_{1k} \cos \phi - x_{2k} \sin \phi)/\sqrt{R} \right) \right] \right\} \\ & - \mathbf{E} \left\{ R(a_k \cos \phi - b_k \sin \phi) f \left[R \left(a_k \sin \phi + b_k \cos \phi + (-x_{1k} \sin \phi + x_{2k} \cos \phi)/\sqrt{R} \right) \right] \right\} \end{aligned} \quad (\text{A-4})$$

where the expectation is taken first over the random data and then over the thermal noise. Using Eq. (A-4), the expected value of the slope of the error signal can be expressed as

$$\begin{aligned} \overline{\epsilon'(0)} \triangleq \left. \frac{d\overline{\epsilon(\phi)}}{d\phi} \right|_{\phi=0} = & R \mathbf{E} \left\{ a_k f \left[R(a_k - x_{1k}/\sqrt{R}) \right] + b_k f \left[R(b_k + x_{2k}/\sqrt{R}) \right] \right\} \\ & + R^2 \mathbf{E} \left\{ b_k f' \left[R(a_k - x_{1k}/\sqrt{R}) \right] (-b_k - x_{2k}/\sqrt{R}) \right\} \\ & - R^2 \mathbf{E} \left\{ a_k f' \left[R(b_k + x_{2k}/\sqrt{R}) \right] (a_k - x_{1k}/\sqrt{R}) \right\} \end{aligned} \quad (\text{A-5})$$

Averaging the above equation over the random data, one obtains

$$\overline{\epsilon'(0)} = 2Rf[R - \sqrt{R}x] - 2R^2f'[R - \sqrt{R}x] \quad (\text{A-6})$$

where the overbar denotes expectation over the Gaussian random variable x with zero mean and unit variance. After some algebra, we find the expected value of $\epsilon^2(0)$, namely,

$$\mathbf{E}\{\epsilon^2(0)\} = 2R \left[(R+1)\mathbf{E}\{f^2[R - \sqrt{R}x]\} - \left(\mathbf{E}\{xf[R - \sqrt{R}x]\} - \sqrt{R}\mathbf{E}\{f[R - \sqrt{R}x]\} \right)^2 \right] \quad (\text{A-7})$$

In order to proceed further, the non-linearity $f(x)$ needs to be specified. For example, $f(x) = \text{sgn}(x)$ ($f'(x) = 2\delta(x)$) for the Costas cross-over loop, in which case we obtain

$$\mathbf{E}\{\text{sgn}(R - \sqrt{R}x)\} = \text{erf}\left(\sqrt{R/2}\right) \quad (\text{A-8a})$$

$$\mathbf{E}\{2\delta(R - \sqrt{R}x)\} = \sqrt{\frac{2}{\pi R}} e^{-R/2} \quad (\text{A-8b})$$

$$\mathbf{E}\{x \text{sgn}(R - \sqrt{R}x)\} = -\sqrt{\frac{2}{\pi}} e^{-R/2} \quad (\text{A-8c})$$

$$\mathbf{E} \text{sgn}^2(R - \sqrt{R}x) = 1 \quad (\text{A-8d})$$

which result in

$$S_L = \frac{\left[\text{erf} \sqrt{R/2} - \sqrt{\frac{2R}{\pi}} e^{-R/2} \right]^2}{R+1 - \left(\sqrt{R} \text{erf} \sqrt{R/2} + \sqrt{\frac{2}{\pi}} e^{-R/2} \right)^2} \quad (\text{A-9})$$

On the other hand, for the generalized Costas loop, $f(x) = x^3$ ($f'(x) = 3x^2$) and we have

$$\mathbf{E}\{(R - \sqrt{R}x)^3\} = R^2(R+3) \quad (\text{A-10a})$$

$$\mathbf{E}\{3(R - \sqrt{R}x)^2\} = 3R(R+1) \quad (\text{A-10b})$$

$$\mathbf{E}\{x(R - \sqrt{R}x)^3\} = -R^{3/2}(R+1) \quad (\text{A-10c})$$

$$\mathbf{E}\{f^2(x)\} = R^3(R^3 + 15R^2 + 45R + 15) \quad (\text{A-10d})$$

$$S_L = \frac{1}{1 + \frac{9}{2R} + \frac{6}{R^2} + \frac{3}{2R^3}} \quad (\text{A-11})$$

In the MAP estimation loop, the nonlinearity is given by $f(x) = \tanh(x)$ ($f'(x) = \text{sech}^2(x)$), which prevents a closed-form expression, i.e.,

$$S_L = \frac{\left[\overline{\tanh(R - \sqrt{R}x)} - R \overline{\text{sech}^2(R - \sqrt{R}x)} \right]^2}{(R+1) \overline{\tanh^2(R - \sqrt{R}x)} - \left[x \overline{\tanh(R - \sqrt{R}x)} - \sqrt{R} \overline{\tanh(R - \sqrt{R}x)} \right]^2} \quad (\text{A-12})$$

The variance of the phase error process in all three loops can be expressed as

$$\sigma_\phi^2 = \frac{N'_0 B_L}{[\epsilon'(0)]^2} = \frac{1}{\rho_c S_L} = \frac{B_L}{r_{sy} R S_L} \quad (\text{A-13})$$

where $\rho_c \triangleq \frac{P_D}{N'_0 B_L}$, B_L is the loop bandwidth, r_{sy} is the symbol rate, and $R = E_s/N_0$ is the symbol SNR. Note that for $R \approx 1$ dB, $S_L \ll 1$. We should comment that the above variance σ_ϕ^2 is the variance relative to ω_0 , which is used to compute the telemetry performance. The variance that determines acquisition and the cycle slip process is relative to $4\omega_0$, and hence will be 16 times larger.

Appendix B

Error and Detector Signals for MPSK

Let r_c be the “in-phase” and r_s the “quadrature” outputs of the integrate-and-dump devices of a MPSK loop: Ref. [4] proposes the following algorithms for deriving the error signal and the detector’s signals for the various MPSK tracking loops.

Derivation algorithms		
M	Error signal	Detector signal
2	$\epsilon_2 = r_c \times r_s$	$d_2 = r_c^2 - r_s^2$
4	$\epsilon_4 = d_2 \times \epsilon_2$	$d_4 = d_2^2 - \epsilon_2^2$
8	$\epsilon_8 = d_4 \times \epsilon_4$	$d_8 = d_4^2 - \epsilon_4^2$
N	$\epsilon_N = d_{\frac{N}{2}} \times \epsilon_{\frac{N}{2}}$	$d_N = d_{\frac{N}{2}}^2 - \epsilon_{\frac{N}{2}}^2$

Appendix C

QPSK Lock-Detector Statistics

The signal for the lock detector is derived using the following algorithm

$$z = \sum_k^M y_k \gtrless \tau$$

where

$$y_k \triangleq (r_{ck}^2 - r_{sk}^2)^2 - (2r_{ck}r_{sk})^2 \quad (\text{C-1})$$

In order to compute the mean and the variance of z , we need the second through the eighth moments of r_{ck} and r_{sk} . The odd moments are all zero (since the noise is Gaussian), and hence only the even moments need to be computed. To simplify the notation, the subscript k will be dropped from the next several equations. Taking the expected value of Eq. (4), the even moments are given by

$$m_2 \triangleq \overline{r_c^2} = \overline{r_s^2} = R^2 \left(1 + \frac{1}{R} \right) \quad (\text{C-2})$$

$$m_4 \triangleq \overline{r_c^4} = \overline{r_s^4} = R^4 \left(r - \frac{1}{2} \overline{\cos 4\phi} \right) \quad (\text{C-3})$$

$$m_6 \triangleq \overline{r_c^6} = \overline{r_s^6} = R^6 \left(\frac{1}{2} (5 - 3 \overline{\cos 4\phi}) + \frac{15}{2R} (3 - \overline{\cos 4\phi}) + \frac{15}{R^2} \left(3 + \frac{1}{R} \right) \right) \quad (\text{C-4})$$

$$\begin{aligned} m_8 \triangleq \overline{r_c^8} = \overline{r_s^8} = R^8 & \left[\frac{1}{16} \left(105 - 5 \overline{\cos 4\phi} - 84 \overline{\cos 4\phi} \right) \right. \\ & \left. + \left(\frac{7}{2R} (5 + 3 \overline{\cos 4\phi}) + 15 (1 - \overline{\cos 4\phi}) \right) \left(\frac{105}{2R^2} (3 + \overline{\cos 4\phi}) + 3 (1 - \overline{\cos 4\phi}) \right) + \frac{420}{R^3} + \frac{105}{R^4} \right] \end{aligned} \quad (\text{C-5})$$

where

$$r = 3 \left(\frac{1}{2} + \frac{2}{R} + \frac{1}{R^2} \right) \quad (\text{C-6})$$

At high-loop SNR, $\phi \rightarrow 0$ and m_4 , m_6 , m_8 reduce to

$$R^4 \left(1 + \frac{6}{R} + \frac{3}{R^2} \right) \quad (\text{C-7})$$

$$R^6 \left(1 + \frac{15}{R} + \frac{45}{R^2} + \frac{15}{R^3} \right) \quad (\text{C-8})$$

$$R^8 \left(1 + \frac{28}{R} + \frac{210}{R^2} + \frac{420}{R^3} + \frac{105}{R^4} \right) \quad (\text{C-9})$$

respectively. Cross-moments for $i = j$ are also needed and are given by

$$m_{22} \triangleq \mathbf{E}\{r_c^2 r_s^2\} = R^4 \left(\frac{1}{2}(1 + \overline{\cos 4\phi}) + \frac{2}{R} + \frac{1}{R^2} \right) \quad (\text{C-10a})$$

$$m_{44} \triangleq \mathbf{E}\{r_c^4 r_s^4\} = R^8 \left(r^2 + \frac{1}{8}(1 + \overline{\cos 8\phi}) - \overline{r \cos 4\phi} - \frac{18}{R^2}(1 - \overline{\cos 4\phi}) \right) \quad (\text{C-10b})$$

$$m_{62} \triangleq \mathbf{E}\{r_s^6 r_c^2\} = \mathbf{E}\{r_c^6 r_s^2\} = R^8 \left(-5 + 6\overline{\cos 4\phi} + \frac{1}{R}(25 - 9\overline{\cos 4\phi}) + \frac{15}{2R}(9 - \overline{\cos 4\phi}) + \frac{60}{R^3} + \frac{15}{R^4} \right) \quad (\text{C-10c})$$

Note that as $\sigma_\phi \rightarrow 0$, $m_{22} \rightarrow m_2^2$, $m_{44} \rightarrow m_4^2$, and $m_{62} \rightarrow m_6 m_2$. Now, the mean value and the variance of the detector's signal can be computed. The mean is given by

$$\mu_z = \sum_{k=1}^M \mathbf{E}\{y_k\} = M\mu_y \quad (\text{C-11})$$

where

$$\mu_y = \overline{r_c^4} + \overline{r_s^4} - 6\overline{r_c^2 r_s^2} \quad (\text{C-12})$$

Using the moments just obtained gives

$$\mu_y = -4R^4 \overline{\cos 4\phi} \quad (\text{C-13})$$

The next step is to find the moment of z^2 . Equation (C-1) gives

$$\begin{aligned} z^2 &= \left(\sum_{i=1}^M r_{ci}^4 + \sum_{i=1}^M r_{si}^4 - 6 \sum_{i=1}^M r_{ci}^2 r_{si}^2 \right)^2 = \sum_{i=1}^M \sum_{j=1}^M r_{ci}^4 r_{cj}^4 + \sum_{i=1}^M \sum_{j=1}^M r_{si}^4 r_{sj}^4 \\ &\quad + 36 \sum_{i=1}^M \sum_{j=1}^M r_{ci}^2 r_{cj}^2 r_{si}^2 r_{sj}^2 + 2 \sum_{i=1}^M \sum_{j=1}^M r_{ci}^4 r_{sj}^4 - 12 \sum_{i=1}^M \sum_{j=1}^M r_{ci}^4 r_{cj}^2 r_{sj}^2 - 12 \sum_{i=1}^M \sum_{j=1}^M r_{si}^4 r_{cj}^2 r_{sj}^2 \end{aligned} \quad (\text{C-14})$$

Let $z^2 = S_1 + S_2$, where S_1 is the sum of all the terms when $i = j$ and S_2 is the sum of all the terms for $i \neq j$. Then for $i = j$

$$\overline{r_{ci}^4 r_{cj}^4} = \overline{r_{si}^4 r_{sj}^4} = m_8 \quad (\text{C-15a})$$

$$\overline{r_{ci}^4 r_{sj}^4} = m_{44} \quad (\text{C-15b})$$

$$\overline{r_{ci}^6 r_{sj}^2} = \overline{r_{si}^6 r_{cj}^2} = m_{62} \quad (\text{C-15c})$$

and

$$S_1 = 2M(m_8 + 19m_{44} - 12m_{62}) \quad (\text{C-16})$$

For $i \neq j$, let $k \triangleq |i - j|$. Note that $\overline{r_{ci}^2 r_{cj}^2} = m_2^2$ because the random data make the second moments of r_{ci}^2 independent of r_{cj}^2 . The double sums can be converted into single sums as follows:

$$\begin{aligned} S_2 &= 2 \sum_{k=1}^{M-1} c_k \overline{r_{ci}^4 r_{cj}^4} + 36 \sum_{k=1}^{M-1} c_k \overline{r_{ci}^2 r_{cj}^2 r_{si}^2 r_{sj}^2} + 2 \sum_{k=1}^{M-1} c_k \overline{r_{ci}^4 r_{sj}^4} - 24 \sum_{k=1}^{M-1} c_k \overline{r_{ci}^4 r_{cj}^2 r_{sj}^2} \\ &= 4 \sum_{k=1}^{M-1} c_k d_k + 36(M-1)Mm_2^4 - 24(M-1)Mm_4m_2^2 \end{aligned} \quad (C-17)$$

where $c_k = 2(M - k)$ for $k = 1, 2, \dots, M - 1$. Note that $\sum_{k=1}^{M-1} c_k = M^2 - M$ (and $c_0 = M$). The variance of z can now be found from the relation

$$\sigma_z^2 = \overline{z^2} - (\bar{z})^2 = S_1 + S_2 - \mu_z^2 \quad (C-18)$$

Using the previous equations, it can be shown that

$$\sigma_z^2 = 2M \left[m_8 + 19m_{44} - 12m_{62} \right] + 4M \left[\frac{1}{M} \sum_{k=1}^{M-1} c_k d_k - Mm_4^2 - 9m_2^4 + 6m_4m_2^2 \right] \quad (C-19)$$

where

$$d_k \triangleq \overline{x_{ci}^4 x_{cj}^4}$$

such that

$$\begin{aligned} k &= |i - j| \\ &= \overline{\left(r - \frac{1}{2} \cos 4\phi_i \right) \left(r - \frac{1}{2} \cos 4\phi_j \right)} \\ &= (r^2 - re^{-8\sigma_\phi^2} + f_k/4) \end{aligned} \quad (C-20)$$

and

$$f_k \triangleq \overline{\cos 4\phi_i \cos 4\phi_j} \quad (C-21)$$

At high-loop SNR, the mean and variance become

$$\mu_{z,ideal} = -4MR^4 \quad (C-22a)$$

and

$$\sigma_{z,ideal}^2 = 64MR^8 \left(\frac{2}{R} + \frac{9}{R^2} + \frac{12}{R^3} + \frac{3}{R^4} \right) \quad (C-22b)$$

which result in

$$SNR_{z,ideal} = \frac{MR}{4(2 + \frac{9}{R} + \frac{12}{R^2} + \frac{3}{R^3})} \quad (C-23)$$

So far, no assumption has been made regarding the statistics of the phase error process. Assuming that the phase error is indeed Gaussian with second-order density,

$$\begin{aligned} p(\phi_i, \phi_j, \tau) &\approx \frac{1}{2\pi\sqrt{R^2(0) - R^2(\tau)}} \exp\left(-\frac{R(0)\phi_i^2 - 2R(\tau)\phi_i\phi_j + R(0)\phi_j^2}{2(R^2(0) - R^2(\tau))}\right) \\ &= \frac{1}{2\pi\sigma_\phi^2\sqrt{1 - C^2(\tau)}} \exp\left(-\frac{\phi_i^2 - 2C(\tau)\phi_i\phi_j + \phi_j^2}{2\sigma_\phi^2(1 - C^2(\tau))}\right) \end{aligned} \quad (C-24)$$

where $R(\tau)$ is the correlation function and can be expressed in terms of the normalized correlation function $C(\tau)$ as $R(\tau) = \sigma_\phi^2 C(\tau)$ where

$$C(\tau_k) = \left(1 - \frac{|B_L \tau_k|}{0.91}\right) \exp(-1.25 B_L \tau_k) \quad (C-25)$$

B_L is the one-sided loop bandwidth and σ_ϕ^2 the closed-loop error variance.

$$\tau_k \triangleq \tau_{ij} = T_s |i - j| = |t_i - t_j| \quad (C-26)$$

With this Gaussian assumption, the expected value of $\cos b\phi$ will be $e^{\frac{-b^2\sigma_\phi^2}{2}}$. Hence, we can substitute in all the above equations $\overline{\cos 4\phi}$ with $e^{-8\sigma_\phi^2}$ and $\overline{\cos 8\phi}$ with $e^{-32\sigma_\phi^2}$. Moreover,

$$\overline{\cos 4\phi_i \cos 4\phi_j} = e^{-16\sigma_\phi^2} \cosh(16\sigma_\phi^2 C(\tau_k)), \quad i \neq j \quad (C-27)$$